Acta Materialia 113 (2016) 180–193

Contents lists available at ScienceDirect

Acta Materialia

journal homepage: www.elsevier.com/locate/actamat

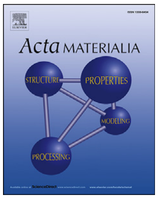

Full length article

Iterative thermomechanical processing of alloy 600 for improved resistance to corrosion and stress corrosion cracking

Abhishek Telang [a], Amrinder S. Gill [b], Mukul Kumar [c], Sebastien Teysseyre [d], Dong Qian [e], Seetha R. Mannava [a], Vijay K. Vasudevan [a, *]

[a] Department of Mechanical and Materials Engineering, University of Cincinnati, Cincinnati, OH 45221-0072, USA
[b] AK Steel, Research Center, 705 Curtis Street, Middletown, OH, USA
[c] Lawrence Livermore National Laboratory, Livermore, CA, USA
[d] Idaho National Laboratory, Idaho Falls, ID, USA
[e] The University of Texas at Dallas, Richardson, TX, USA

ARTICLE INFO

Article history:
Received 15 March 2016
Accepted 5 May 2016

Keywords:
EBSD
Corrosion
Stress corrosion cracking
Grain boundary
Thermo-mechanical processing

ABSTRACT

The effects of thermomechanical processing (TMP) with iterative cycles of 10% cold work and strain annealing, on corrosion and stress corrosion cracking (SCC) behavior of alloy 600 was studied. The associated microstructural and cracking mechanisms were elucidated using transmission (TEM) and scanning electron microscopy (SEM), coupled with precession electron diffraction (PED) and electron back scatter diffraction (EBSD) mapping. TMP resulted in increased fraction of low coincident site lattice (CSL) grain boundaries whilst decreasing the connectivity of random high angle grain boundaries. This disrupted random grain boundary network and large fraction of low CSL boundaries reduced the propensity to sensitization, i.e. carbide precipitation and Cr depletion. After TMP, alloy 600 (GBE) also showed higher intergranular corrosion resistance. Slow strain rate tests in 0.01 M $Na_2S_4O_6$ solution at room temperature show TMP lowered susceptibility to intergranular SCC. To better understand the improvements in corrosion and SCC resistance, orientation maps of regions around cracks were used to analyze the interactions between cracks and various types of grain boundaries and triple junctions (TJs). Detailed analysis showed that cracks were arrested at J1 (1-CSL) and J2 (2-CSL) type of TJs. The probability for crack arrest at special boundaries and TJs, calculated using percolative models, was found to have increased after TMP, which also explains the increase in resistance to corrosion and SCC in GBE alloy 600. A clear correlation and mechanistic understanding relating grain boundary character, sensitization, carbide precipitation and susceptibility to corrosion and stress corrosion cracking was established.

1. Introduction

Grain boundary engineering (GBE) has been demonstrated as a viable method for improving the resistance to corrosion [1–3] and stress corrosion cracking (SCC) [4–8] in austenitic stainless steels (SS) and Ni based alloys (alloy 600, alloy 690). GBE involves increasing the frequency of coincident site lattice (CSL) grain boundaries whilst disrupting the random grain boundary network through thermo-mechanical processing (TMP) routes. These routes involve cold rolling or uniaxial tension/compression followed by annealing and have been used to increase the frequency of CSL boundaries [1,3,9–11]. One approach involves pre-straining the material followed by annealing at comparatively lower temperature for a long time (24–72 h). Another multi-cycle approach uses two or more iterations of cold work (6–30%) followed by relatively high temperature annealing for short times (10–30 min) and has also been shown to increase the low CSL boundary fraction [11,12]. In addition, the multi-cycle approach results in numerous disruptions in the random high angle grain boundary (HAB) network. Further, a significant improvement in the corrosion and stress corrosion cracking has been attributed to these changes in the microstructure [13,14].

Alloy 600 and austenitic stainless steels have been known to be susceptible to SCC in polythionic acid environments [15–18]. Susceptibility to SCC at low temperature in tetrathionate and thiosulfate environments has been attributed to Cr depletion in the area

---

[*] Corresponding author.
E-mail address: vijay.vasudevan@uc.edu (V.K. Vasudevan).

http://dx.doi.org/10.1016/j.actamat.2016.05.009
1359-6454/

surrounding the grain boundary. A reduction in Cr depletion by disrupting the random grain boundary network or increasing the fraction of special/low CSL boundaries decreases the susceptibility to SCC [19].

Twin boundaries are more resistant to carbide precipitation and corrosion because the atomic structure is highly coherent as compared with high angle grain boundaries. In particular, Σ3 and Σ9 boundaries in GBE SS304 have been observed to be more resistant to sensitization, whereas Σ27 and other CSL boundaries were not really "special" in terms of their resistance to sensitization and thus intergranular stress corrosion cracking (IGSCC). Thus, it has been suggested that increased fraction of Σ3 and Σ9 and other low CSL boundaries would likely improve the corrosion and SCC resistance [20–23].

The purpose of this study was to evaluate the susceptibility of grain boundaries of known character to intergranular corrosion and their resistance to SCC. In this study, we use multi-step TMP to increase the fraction of low CSL boundaries. Electron back-scattered diffraction (EBSD) is used to characterize changes in the microstructure after TMP. Transmission Electron microscopy (TEM) and Precession Electron Diffraction (PED) were also used to characterize the microstructure and precipitation of carbides after sensitization. Double loop Electrochemical Potentiokinetic Reactivation (DLEPR) and intergranular corrosion tests were used to evaluate the corrosion resistance. We also performed slow strain rate tests to evaluate the susceptibility to intergranular SCC after TMP. EBSD mapping of regions around crack tips after DLEPR tests, corrosion (ASTM G28) tests and interrupted slow strain rate tests (SSRTs) were used to study the interaction of cracks with various types of boundaries and triple junctions to explain the improvements in grain boundary engineered Alloy 600.

2. Materials and methods

2.1. Thermo-mechanical processing and characterization

Alloy 600 plate (2 mm thickness) with chemical composition as shown in Table 1 was given an annealing treatment at 1050 °C for 10 min and then water quenched (WQ). For TMP, these plates were cold rolled 10% and subsequently annealed in a furnace for 10 min at 900 °C or 1000 °C, then water quenched. This cycle was repeated 3 times to obtain 2 heats of thermo-mechanically processed Alloy 600, designated GBE1 and GBE2. Processing details for all conditions are listed in Table 2.

For EBSD, each coupon was electropolished in 12.5:87.5 sulfuric acid to methanol solution at 24 V, 10s and finally polished with 0.05 μm colloidal silica suspension. EBSD orientation mapping was performed in a FEI XL-30 scanning electron microscope (SEM) with step size of 0.5–1.5 μm at 30 kV. OIM scans were analyzed with the TSL OIM Analysis 7 package to calculate grain boundary character distribution, grain size, and types of triple junctions. CSL grain boundaries were categorized according to the Brandon criterion of $\Delta\theta \leq 15^\circ\Sigma^{-1/2}$ [24]. Boundaries with $3 < \Sigma < 29$ were considered to be CSL boundaries, whereas boundaries with $\Sigma > 29$ were considered HABs and $\Sigma = 1$ as low angle boundaries (LABs) [25]. Triple junctions (TJs) with no CSL boundaries, 1 CSL boundary, 2 CSL and 3 CSL boundaries have been classified as J0, J1, J2 and J3 junctions, respectively. For TJ analysis, only Σ3, Σ9 and Σ27 were considered as CSL boundaries.

Table 2
Designation and corresponding processing details for conditions used in this study.

Designation	Detail
SA	As received + Annealing at 1050 °C, 10 min, WQ
GBE1	SA + 3 cycles of (10% cold work + 1000 °C,10 min,WQ)
GBE2	SA + 3 cycles of (10% cold work + 900 °C,10 min,WQ)

TEM was used to characterize the precipitation behavior of carbides on grain boundaries of known character. Thin foils were prepared by conventional method including grinding, dimpling and finally ion-milling. Foils were obtained from SA and GBE1 samples after sensitization (650 °C, 2 h) and analyzed with a Philips/FEI CM-20 TEM operating at 200 kV. Nanoscale lateral spatial resolution OIM analysis was performed by automated acquisition and indexing of precession electron diffraction (PED) patterns with a JEM 2100F TEM equipped with the DIGISTAR/ASTAR system from NanoMEGAS at the University of Pittsburgh. Precessed illumination, 0.6° precession angle, and electron beam focused to ~3 nm in diameter at the TEM specimen section surface was scanned across a pre-selected area of interest with step-size of 20 nm to obtain maps of PED patterns, which were indexed automatically by optimized matching to computer generated reciprocal lattice based templates of the Nickel and Cr_7C_3 (carbide) phases of interest here. The PED based TEM OIM data sets provide information akin to that available via EBSD based OIM in the SEM but with lateral resolution in areal maps being on the order of 2 nm, limited essentially by the electron beam diameter used in the TEM instrument. The raw data sets of the PED based orientation indexed areal maps were processed and analyzed further with the TSL OIM Data Analysis software.

2.2. Double loop electrochemical potentiokinetic reactivation (DLEPR) and corrosion tests

All samples (SA, GBE1 and GBE2) were given a sensitization treatment in a laboratory furnace at 650 °C, 2 h and water quenched (WQ) to induce precipitation of carbides at grain boundaries, and hence depletion of Cr from the surrounding regions. These samples were mechanically ground to 1200 grit, wet polished with 1 μm diamond suspension and finished with 0.05 μm colloidal silica suspension. DLEPR tests were performed in a solution composed of 0.01 M H_2SO_4 + 20 ppm KSCN using a Gamry Potentiostat (Reference 600) [26,27]. The scan rate was set at 0.5 mV/s for activation and reactivation loop and the sampled area size was 1 cm^2. Freshly prepared solution was de-aerated with high purity Argon gas before and during each test and all tests were performed at room temperature. Samples were kept immersed in the test solution for 1 h at open circuit potential before the start of each test. The following procedure was used to quantify sensitization in the annealed and GBE material after sensitization [28].

The degree of sensitization is reported as DL-EPR value (designated as R in %) which is the ratio of the current density in the reactivation loop to that in the activation loop times 100.

$$R = \frac{Ir}{Ia} \times 100 \qquad (1)$$

Table 1
Chemical composition of the Inconel alloy 600 used in this study.

C	Mn	Si	S	Cr	Fe	Co	Cd	Ti	Cu	P	Al	Ni
0.08	0.16	0.18	0.001 max.	14.99	8.05	0.18	0.01	0.18	0.1	0.001 max.	0.08	Bal.